frontiers | Frontiers in Earth Science

ORIGINAL RESEARCH
published: 17 June 2022
doi: 10.3389/feart.2022.950626

The Discovery and Geochemical Characteristics of an Eocene Peridotite Xenolith-Bearing Mafic Volcanic Neck in Coastal Southeast China

Chuanshun Li[1], Xilin Zhao[2,3,4], Yang Jiang[2], Guangfu Xing[2], Minggang Yu[2] and Zheng Duan[2]*

[1]First Institute of Oceanography, Ministry of Natural and Resources, Qingdao, China, [2]Nanjing Center, China Geological Survey, Nanjing, China, [3]Research Center for Petrogenesis and Mineralization of Granitoid Rocks, China Geological Survey, Wuhan, China, [4]School of Resources and Environmental Engineering, Hefei University of Technology, Hefei, China

The mantle beneath coastal SE China evolved from enriched to depleted between the Cretaceous and the Neogene, although the precise timing of this change remains unclear. Here, we focus on a newly discovered Eocene mafic volcanic neck that contains peridotite xenoliths in the Fuding area of Fujian Province, and present new whole-rock Ar–Ar data which indicate that flood basalts formed during the Eocene (ages of 38.5 ± 1.2 and 42.3 ± 2 Ma). The basalt, gabbro, and diabase in the Fuding area are geochemically similar to ocean island basalt (OIB) and have Sr_I values that range from 0.703794 to 0.703911 (average of 0.703865) and εNd(t) values from 3.05 to 4.56 (average of 3.90). These samples yield two-stage Nd model (T_{DM2}) ages of 0.61–0.73 Ga (average of 0.67 Ga). These data indicate that all of these units formed from magmas derived from an OIB-type mantle source, with both the gabbro and diabase units recording minor amounts of crustal contamination. Its OIB type geochemical characteristics may be inherited from crustal materials with similar characteristics. Peridotite xenoliths within the Fuding basalts provide evidence of the nature of the Eocene mantle in this area, especially the post late-Mesozoic evolution of the mantle beneath coastal SE China. The mantle beneath coastal SE China evolved from enriched in the Cretaceous to depleted in the Neogene, with this change occurring during the Eocene.

Keywords: coastal SE China, eocene, mafic volcanic neck, peridotite xenolith, whole-rock Ar-Ar

OPEN ACCESS

Edited by:
Fuhao Xiong,
Chengdu University of Technology, China

Reviewed by:
Chenyue Liang,
Jilin University, China
Weimin Li,
Jilin University, China

****Correspondence:***
Xilin Zhao
zxl24@126.com

Specialty section:
This article was submitted to Petrology, a section of the journal Frontiers in Earth Science

Received: *23 May 2022*
Accepted: *31 May 2022*
Published: *17 June 2022*

Citation:
Li C, Zhao X, Jiang Y, Xing G, Yu M and Duan Z (2022) The Discovery and Geochemical Characteristics of an Eocene Peridotite Xenolith-Bearing Mafic Volcanic Neck in Coastal Southeast China. Front. Earth Sci. 10:950626. doi: 10.3389/feart.2022.950626

1 INTRODUCTION

Continental lithosphere is an important component of the Earth, and peridotite xenoliths captured by rapidly ascending basaltic magmas produced in some tectonic environments can provide direct samples of the upper mantle or lower crust of continental lithosphere. Such xenoliths also provide evidence of the nature and evolution of the mantle, the composition of the mantle, and the tectonic setting of the basaltic magmatism that captured the xenoliths. There are two main models for the petrogenesis of peridotite xenoliths: 1) they represent the refractory residue of the upper mantle after partial melting that generated basaltic magmas (Wang and Yang, 1987a; Wang and Yang., 1987b; Deng et al., 1988; Cong et al., 1996; Yan et al., 2007), or 2) they represent rock fragments of the upper mantle that were captured by ascending basaltic magma as accidental enclaves, meaning they played no direct role in the formation of the basaltic magmas (Tatsumoto et al., 1992; C. ; Liu et al., 1995; T. ; Li and Ma, 2002).

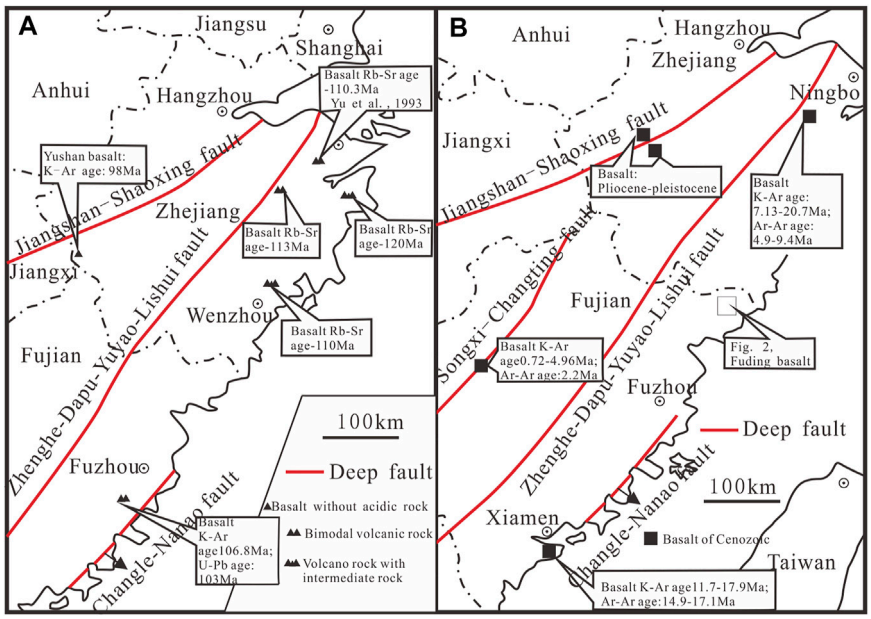

FIGURE 1 | Temporal and spatial distribution of late Mesozoic–Cenozoic basalts in SE China (revised after Xu and Xie, 2005). **(A)** Temporal and spatial distribution of late Mesozoic basalts in SE China; **(B)** Temporal and spatial distribution of Cenozoic basalts in SE China.

Southeastern China has a complex geological history that includes late Mesozoic to Cenozoic lithospheric thinning and extensive basaltic magmatism. This magmatism peaked in coastal SE China after the late Mesozoic and has been the focus of many studies (Cui et al., 2011; C. ; Liu et al., 1995; Tang et al., 2010; G. ; Xie et al., 2005; Xing et al., 1999; J. ; Yan et al., 2005a; Zhou et al., 2006), including a large body of research devoted to the nature of the mantle during this magmatism (D. Chen et al., 1997; C. Chen et al., 2008; C. Dong C. W. et al., 2006; C. Dong Y. X. et al., 2006; He and Xu, 2011; Li, 2000; Z. Li and Li, 2007; X. Li et al., 2007; J. Liu and Yan, 2007; Shen et al., 1999; D. Y. Wang et al., 2002; D.Z. Wang and Shen, 2003; Xiao et al., 2006; X. Xu et al., 2008; W. Zhang and Fang, 2014; Zhi and Qin, 2004; Zhi et al., 1994). This previous research focused on the Late Cretaceous and Miocene mantle in this area and was based on mantle xenoliths obtained mainly from late Neogene basaltic rocks. Peridotite xenoliths also occur within post-Neogene alkaline basalts that have been used to characterize the Cenozoic evolution of the mantle beneath SE China (Bodinier and Garrido, 2008; C. ; Dong et al., 1997; Z. ; Dong et al., 1999; X. ; Wang et al., 2012).

However, the Paleogene (and especially the Eocene) evolution of the mantle in this area is poorly known, primarily due to the rarity of basic rocks hosting mantle xenoliths that formed at this time, meaning that the characteristics and the evolution of the Cretaceous to Neogene mantle beneath coastal SE China are uncertain.

Rare peridotite xenoliths are present within Mesozoic and Paleogene basalts in coastal SE in China (**Figure 1**), including peridotite xenoliths within Mesozoic basalts of the Fuxin area of Liaoning Province, the Daoxian area in Hunan Province, and the Daxizhuang area of eastern Shandong Province (Guo et al., 2013a; Guo et al., 2013b; Pei et al., 2004; D. Y. ; Wang et al., 2002; Xia et al., 2010; W. ; Xu et al., 2013; J. ; Yan et al., 2005a; G. ; Yang et al., 2012; J. ; Ying et al., 2010; J. ; Ying et al., 2013; X. ; Yang et al., 2008; Zheng et al., 1999; Q.J. ; Zhou et al., 2013). Previous research on this Mesozoic mantle has been based on inference, meaning the characteristics of this mantle source region are poorly constrained.

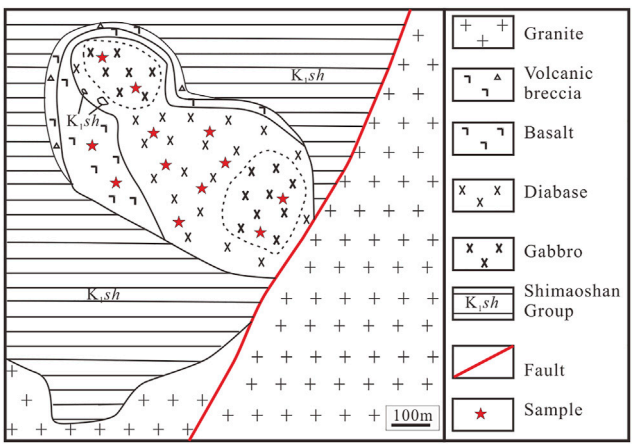

FIGURE 2 | Tectonic and geological maps of the Fuding area, Fujian province (adapted from Dai and Chen, 2008).

A mafic volcanic neck located in the Fuding area of coastal SE China, within the southern section of the Cretaceous Fuding volcanic basin, is associated with a Mesozoic tectono-magmatic belt that is controlled by the NE–SW striking Fuding–Fuqing

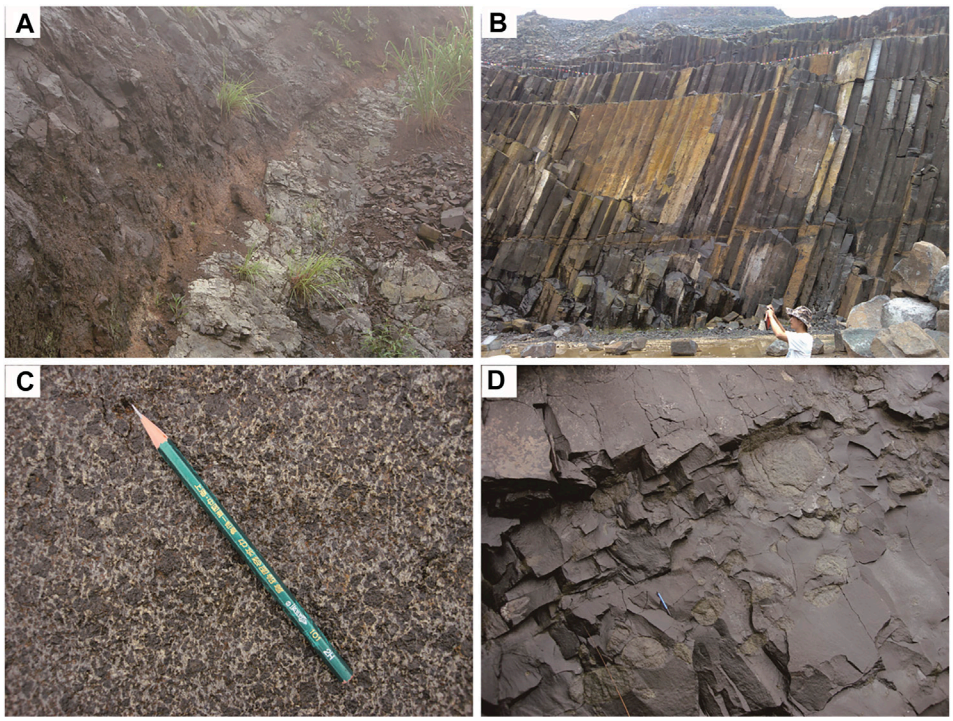

FIGURE 3 | Photographs showing typical characteristics of the Fuding mafic volcanic neck. **(A)** Contact between basalts and units of the Shimaoshan Group, showing a maroon baked margin, **(B)** columnar-jointed gabbro and diabase, **(C)** general characteristics of the cumulate-textured Fuding gabbro, **(D)** rounded peridotite xenoliths within the layered basalt.

Fault. The Fuding basalts were erupted onto volcanic rocks of the lower Shimaoshan Formation (**Figure 2**), contain peridotite xenoliths, and were assigned by L. Li et al. (2011) to the late Oligocene to middle Pleistocene Fotan Group.

Here, we present new whole-rock Ar–Ar ages and geochemical data for mafic rocks from the Fuding mafic volcanic neck. These data constrain the formation age and tectonic setting of the Fuding mafic rocks, which contain peridotite xenoliths that provide clues to the characteristics of the Eocene mantle and to the post late-Mesozoic evolution of the mantle in coastal SE China.

2 GEOLOGICAL BACKGROUND AND PETROLOGICAL CHARACTERISTICS

The Fuding mafic volcanic neck is oval shaped and has a long axis that trends NW–SW, with a length of 790 m, a width of 420 m (**Figure 2**), and with clearly developed columnar joints. The neck is divided into three facies: an outermost eruption facies basaltic breccia volcano, an intermediate effusive facies basalt, and an innermost central neck facies volcano containing olivine-bearing gabbro–diabase rocks (**Figure 3A**). The neck contains basaltic volcanic breccias, basalts, gabbros, and diabasic rocks. The lithofacies within the neck are heterogeneously distributed, with a columnar jointed cumulate gabbro section located above the diabase (**Figures 3B,C**). The geological characteristics of the neck are as follows.

2.1 Volcanic Breccia

The volcanic breccias are gray–black, are brecciated and massive, and are dominated by breccias and crystals in a basaltic matrix. The rocks comprise angular–subangular breccia (60%–70% of the rock mass), and crystals (10%) of olivine, clinopyroxene, spinel, and others (**Figure 4A**) in a basaltic matrix (20%) containing skeletal crystals.

2.2 Basalt

The basalt is gray–black, porphyritic, and has an almond-shaped structure. These rocks contain olivine (0.3–3 mm in size), clinopyroxene, and plagioclase phenocrysts that form 10%–20% of the rock. The amygdales in the basalt are filled with zeolite (**Figures 4B,C**), and both amygdales and phenocrysts are hosted by an intergranular matrix that contains clinopyroxene (50%–55%), olivine (5%), feldspar (12%–15%), basaltic glass (15%), and minor ilmenite. The presence of basaltic glass indicates that the basaltic magma underwent rapid cooling to form a rock with minor amounts of iddingsite and chlorite alteration.

These basalts contain many rounded peridotite xenoliths (**Figure 3D**) that are generally 3–15 cm across (largest, 20 cm). The xenoliths are spinel lherzolites with a subhedral granular

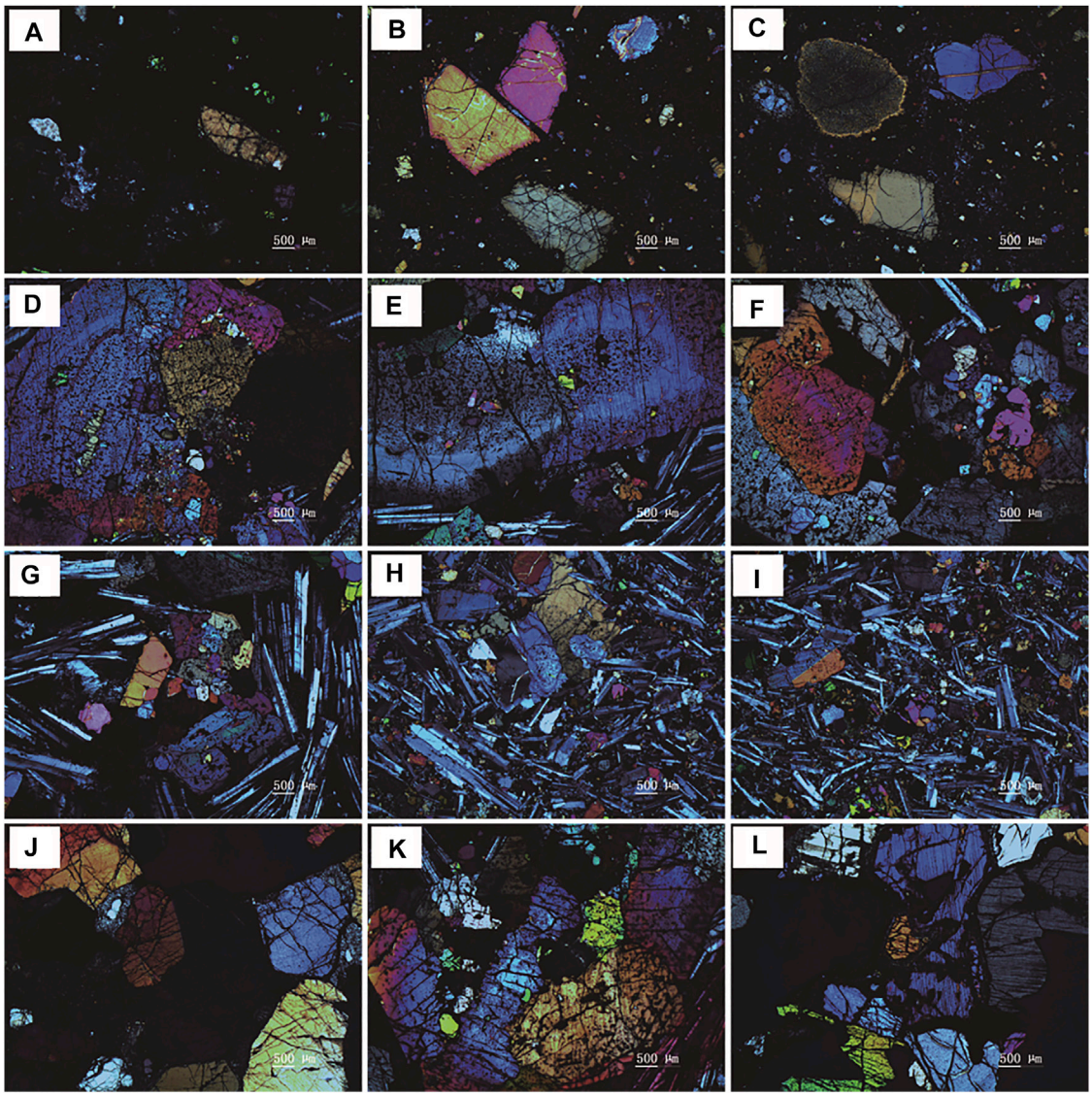

FIGURE 4 | Representative photomicrographs showing typical petrographic features of the Fuding mafic volcanic neck. **(A)** Typical basaltic breccia, **(B)** olivine and clinopyroxene phenocrysts within basalt, **(C)** olivine phenocrysts within vesicular basalt, **(D)** clinopyroxene phenocrysts overprinting olivine within cumulate-textured gabbro, **(E)** zoned clinopyroxene phenocrysts within cumulate-textured gabbro, **(F)** diabasic textured diabase, **(G)** diabasic and intersertal textured diabase, **(H)** diabasic textured diabase, **(I)** diabasic textured diabase containing twinned clinopyroxene, **(J)** granular mosaic textured and zoned clinopyroxene phenocrysts, **(K)** peridotite xenoliths with small olivines enclosed by clinopyroxene, **(L)**: peridotite xenoliths and olivines containing visible kink banding.

texture (**Figures 4J–L**) and they contain olivine (95%) with minor amounts of spinel, clinopyroxene, and orthopyroxene (<5%).

2.3 Gabbro

The gabbro is dark–gray, medium-grained, and has a cumulate gabbroic texture. The largest phenocrysts are ~15 mm in diameter and the rock contains 60%–80% phenocrysts, mainly plagioclase, clinopyroxene, and olivine with minor and localized alkali feldspar. The clinopyroxenes are subhedral, columnar (**Figures 4D,E**), zoned, and make up 15%–20% of the rock, whereas the plagioclase (25%–30%) is euhedral–subhedral and columnar, 0.2–6 mm in size, has clear polysynthetic twinning. The olivine gabbro is subhedral–subhedral, granular, and overprinted by the development of clinopyroxene megacrysts, with some of the olivine being visibly corroded. The olivines have diameters of 0.2–2 mm and make up 10%–20% of the rock. The alkali feldspars are platy and make up 5%–10% of the rock. These minerals occur in a fine-grained matrix of clinopyroxene, olivine, and plagioclase that forms 20%–35% of the rock. The gabbros also contain minor amounts of magnetite, ilmenite, zircon, apatite, and other accessory minerals, and the overall phenocryst abundance within the gabbro unit decreases from top to bottom.

TABLE 1 | Results of $^{40}Ar/^{39}Ar$ dating of Fuding basalt sample TMS2-2.

Power (%)	$^{40}Ar/^{39}Ar$	$^{37}Ar/^{39}Ar$	$^{36}Ar/^{39}Ar$	$^{40}Ar^*/^{39}Ar_k$	$^{40}Ar^*$(%)	^{39}Ark(%)	Age (Ma)	± 2s
Sample name	TMS2-2	groundmass			J = 0.004 650 0 ± 0.000 011 6			
1.5	112.501 99	4.746 41	0.364 51	5.186 578	4.59	3.96	43.09	±23.90
2.0	28.230 86	2.355 78	0.081 00	4.490 241	15.87	21.39	37.37	± 5.00
2.3	11.321 80	1.778 28	0.023 78	4.443 908	39.19	30.21	36.99	± 1.62
2.5	9.599 40	2.068 70	0.017 75	4.527 275	47.08	19.13	37.67	± 1.96
2.8	11.670 14	3.489 24	0.024 22	4.804 107	41.04	7.71	39.95	± 2.54
3.0	11.031 14	2.787 49	0.021 91	4.789 155	43.31	9.74	39.83	± 1.48
3.3	10.380 98	4.863 20	0.019 16	5.127 514	49.19	3.34	42.61	± 2.17
3.8	9.747 77	7.679 70	0.020 28	4.392 694	44.77	1.59	36.56	± 1.75
6.0	11.558 83	28.221 70	0.028 52	5.508 695	46.51	2.20	45.74	± 2.96
9.0	11.050 45	51.606 10	0.027 33	7.402 019	64.04	0.73	61.19	± 4.41

TABLE 2 | Results of $^{40}Ar/^{39}Ar$ dating of Fuding basalt sample TMS2-1.

Power (%)	$^{40}Ar/^{39}Ar$	$^{37}Ar/^{39}Ar$	$^{36}Ar/^{39}Ar$	$^{40}Ar^*/^{39}Ar_k$	$^{40}Ar^*$(%)	^{39}Ark(%)	Age (Ma)	± 2s
Sample name	TMS2-1	groundmass			J = 0.004 650 0 ± 0.000 011 6 (%)			
12	9.918 20	15.160 35	0.023 59	4.205 163	41.85	11.14	35.02	± 8.41
18	10.320 55	24.103 48	0.024 70	5.041 588	47.85	23.27	41.90	± 4.80
23	8.210 10	26.809 99	0.017 64	5.249 289	62.48	65.59	43.61	± 2.13

2.4 Diabase

Diabase occurs beneath the gabbro and has a diabasic texture and a partly visible intersertal texture (**Figures 4F,G**). Some of the clinopyroxenes within the diabase are twinned (**Figures 4H,I**), and this unit has a similar mineralogy to the gabbros described above.

3 ANALYTICAL METHODS

3.1 Whole-Rock Ar–Ar Analytical Procedures

The basalts dated during this study contain peridotite xenoliths and phenocrysts that were removed before analysis. Two basalt samples were dated by whole-rock Ar–Ar methods. The samples were crushed into small chips (≤5 mm) that were hand-picked under a binocular microscope to remove phenocrysts. The $^{40}Ar/^{39}Ar$ dating was carried out using a GV5400 mass spectrometer at the State Key Laboratory of Lithospheric Evolution, Institute of Geology and Geophysics, Chinese Academy of Sciences, Beijing, China, using the analytical procedures described by H. Qiu and Jiang (2007). All errors are reported at 2σ values and argon gas was extracted from the sample by step-heating using a MIR10 CO_2 laser. The released gases were purified using two Zr/Al getter pumps operated for 5–8 min at room temperature and ~450°C, respectively. The background signal prior to analysis was <2 mV and the signal derived from the sample generally fluctuated between 40 and 200 mV. The dating results were calculated and plotted using ArArCALC software (Koppers, 2002), with a J-value of 0.00955 as determined using ZBH-2506 biotite (132 Ma) flux monitors. The results of these Ar–Ar analyses are given in **Tables 1** and **2**.

3.2 Whole-Rock Geochemical Analyses

Bulk-rock major, trace, and rare earth element (REE) concentrations were determined using X-ray fluorescence (XRF) and inductively coupled plasma–mass spectrometry (IC–MS) at the National Research Center for Geoanalysis, Chinese Academy of Geological Sciences (CAGS), Beijing, China. Major element concentrations were determined by XRF and yielded analytical uncertainties better than 5%. Trace and REE concentrations were determined by ICP–MS, with the REE separated using cation exchange techniques. Analytical uncertainties during ICP–MS analysis were 10% for elements with concentrations of <10 ppm and ~5% for those with concentrations of >10 ppm (Zeng et al., 2012). The results of these analyses are listed in **Table 3**.

3.3 Whole-Rock Sr–Nd Isotopic Analyses

Whole-rock Sr and Nd isotope ratios were determined by thermal ionization mass spectrometry (TIMS) using a Finnigan MAT-262 instrument at the CAS Key Laboratory of Crust–Mantle Materials and Environments, University of Science and Technology of China (USTC), Hefei, China. Analytical precision for these isotope ratio measurements is given as ± 2σ (standard error). Sr isotopic ratios were corrected for mass fractionation relative to a $^{86}Sr/^{88}Sr$ value of 0.1194, and analysis of the NBS987 standard yielded a measured $^{87}Sr/^{86}Sr$ ratio of 0.710298 ± 20 with a

TABLE 3 | Major (wt.%) and trace (ppm) compositions of mafic volcanic samples from the northeast of Fujian Province.

Sample	TMS-1-1	TMS-1-2	TMS-1-3	TMS-1-4	TMS-1-5	TMS-2-5	TMS-2-6	TMS-3-1	TMS-3-2	TMS-3-3	TMS-2-1	TMS-2-2
	Gabbro/Diabase										Basalt	
SiO_2	46.54	47.03	46.63	46.73	46.78	46.63	46.60	46.91	46.95	46.86	43.36	44.20
Al_2O_3	12.12	14.23	12.29	13.13	12.86	12.69	12.33	13.01	12.50	13.15	12.01	12.19
Fe_2O_3	2.10	1.75	2.66	2.01	1.77	2.13	1.94	1.70	1.85	2.21	3.26	3.72
FeO	9.01	8.62	8.12	8.85	9.05	9.13	9.33	9.07	9.26	8.65	8.69	7.70
CaO	10.07	8.92	9.95	9.41	9.66	9.28	9.73	9.57	9.60	9.50	8.91	8.51
MgO	10.16	8.64	10.00	9.51	9.60	9.65	10.17	9.36	9.87	9.16	11.12	10.75
Na_2O	2.67	3.30	2.68	2.85	3.01	3.27	2.86	3.17	3.13	3.25	4.46	4.16
K_2O	2.18	2.35	1.99	2.29	2.24	2.26	2.16	2.33	2.04	2.24	2.32	1.90
TiO_2	2.00	1.95	1.97	1.99	1.99	2.05	2.01	2.01	2.00	2.13	2.21	2.09
MnO	0.15	0.14	0.15	0.15	0.15	0.15	0.15	0.15	0.15	0.15	0.17	0.16
P_2O_5	0.65	0.70	0.63	0.67	0.66	0.72	0.66	0.69	0.69	0.73	1.13	1.08
L.O.I	1.78	1.83	2.34	1.84	1.69	1.59	1.62	1.50	1.48	1.52	1.70	2.85
SO_3	0.20	0.22	0.23	0.22	0.20	0.14	0.16	0.17	0.17	0.17	0.23	0.28
Fe_2O_3T	12.13	11.34	11.70	11.86	11.84	12.29	12.32	11.79	12.16	11.84	12.93	12.29
Na_2O+K_2O	4.85	5.65	4.67	5.14	5.25	5.53	5.02	5.50	5.17	5.49	6.78	6.06
FeOT	10.90	10.19	10.51	10.66	10.64	11.05	11.08	10.60	10.92	10.64	11.62	11.05
Mg#	66.13	63.96	66.58	65.14	65.39	64.66	65.79	64.90	65.42	64.33	66.71	67.09
K	18097	19509	16520	19010	18595	18761	17931	19342	16935	18595	19259	15773
Ti	11988	11688	11808	11928	11928	12288	12048	12048	11988	12767	13247	12527
P	2836	3055	2749	2924	2880	3142	2880	3011	3011	3186	4931	4713
AR	1.56	1.65	1.53	1.59	1.61	1.67	1.59	1.64	1.61	1.64	1.96	1.83
Li	5.92	5.55	6.01	5.91	5.51	5.49	5.43	5.75	5.68	6.48	8.60	9.01
Be	1.36	1.53	1.37	1.47	1.44	1.47	1.36	1.48	1.50	1.49	2.24	2.36
Sc	28.30	21.20	27.00	24.00	25.30	22.90	25.60	24.70	26.40	23.20	16.30	17.20
V	217	168	198	184	183	178	193	190	198	183	167	167
Cr	358	206	364	252	292	242	299	282	308	247	526	525

Sample	TMS-1-1	TMS-1-2	TMS-1-3	TMS-1-4	TMS-1-5	TMS-2-5	TMS-2-6	TMS-3-1	TMS-3-2	TMS-3-3	TMS-2-1	TMS-2-2
	Gabbro/Diabase										Basalt	
Co	55	50	52	54	54	51	54	52	54	49	52	53
Ni	164	141	159	154	158	144	158	149	155	136	275	291
Cu	73	75	72	76	75	73	72	76	78	78	63	66
Zn	167	162	160	168	170	161	164	167	171	168	191	192
Ga	20	21	19	20	19	18	18	20	19	20	20	21
Rb	59	60	55	62	65	58	56	66	60	59	68	107
Sr	691	833	627	790	735	652	672	739	692	694	978	991
Y	21.90	21.70	21.30	21.80	21.90	21.50	21.30	22.40	22.90	22.40	23.20	25.10
Nb	55.20	61.20	53.40	58.80	56.00	57.60	54.60	59.10	59.50	60.90	88.90	89.20
Mo	2.02	2.73	2.48	1.96	2.05	2.52	2.02	2.88	2.40	2.93	2.73	2.17
Cd	0.07	0.06	0.07	0.06	0.07	0.06	0.06	0.07	0.08	0.06	0.15	0.18
In	0.07	0.07	0.07	0.07	0.07	0.07	0.07	0.07	0.07	0.07	0.08	0.10
Sb	0.07	0.07	0.06	0.07	0.07	0.06	0.06	0.07	0.07	0.07	0.07	0.11
Cs	0.70	1.21	1.37	0.95	1.15	1.21	1.02	1.06	1.24	1.26	1.37	1.94
Ba	587	680	586	650	624	615	593	659	633	639	758	857
La	47.6	51.9	46.3	50.5	48.8	49.2	46.8	50.9	51.1	50.6	75.9	79.9
Ce	83.5	89.2	80.1	87.2	83.8	84.9	81.0	87.8	88.8	87.6	129.0	136.0
Pr	10.0	10.4	9.4	10.2	9.8	10.0	9.6	10.3	10.5	10.3	15.1	16.0
Nd	40.4	40.9	38.0	40.8	38.8	39.5	38.5	41.1	41.6	40.8	59.3	62.9
Sm	7.83	7.65	7.34	7.72	7.21	7.53	7.37	7.79	7.86	7.72	10.70	11.40
Eu	2.44	2.43	2.28	2.39	2.20	2.29	2.25	2.43	2.44	2.38	3.17	3.30
Gd	6.82	6.55	6.50	6.75	5.96	6.45	6.31	6.75	6.89	6.73	8.60	9.06
Tb	1.16	1.11	1.09	1.14	1.02	1.11	1.08	1.15	1.18	1.14	1.41	1.48
Dy	5.41	5.17	5.07	5.26	4.82	5.11	5.08	5.34	5.48	5.28	5.85	6.35
Ho	0.86	0.82	0.81	0.83	0.79	0.81	0.80	0.85	0.86	0.83	0.85	0.94

Sample	TMS-1-1	TMS-1-2	TMS-1-3	TMS-1-4	TMS-1-5	TMS-2-5	TMS-2-6	TMS-3-1	TMS-3-2	TMS-3-3	TMS-2-1	TMS-2-2
	Gabbro/Diabase										Basalt	
Er	2.24	2.15	2.10	2.19	2.07	2.12	2.08	2.21	2.24	2.16	2.21	2.44
Tm	0.30	0.29	0.28	0.29	0.28	0.28	0.28	0.30	0.30	0.29	0.26	0.30
Yb	1.76	1.71	1.67	1.74	1.67	1.69	1.65	1.75	1.79	1.72	1.54	1.77

(Continued on following page)

TABLE 3 | (*Continued*) Major (wt.%) and trace (ppm) compositions of mafic volcanic samples from the northeast of Fujian Province.

Sample	TMS-1-1	TMS-1-2	TMS-1-3	TMS-1-4	TMS-1-5	TMS-2-5	TMS-2-6	TMS-3-1	TMS-3-2	TMS-3-3	TMS-2-1	TMS-2-2
	Gabbro/Diabase										Basalt	
Lu	0.24	0.24	0.23	0.24	0.23	0.23	0.23	0.24	0.25	0.24	0.21	0.24
Ta	2.64	2.85	2.49	2.74	2.49	2.65	2.52	2.75	2.78	2.76	4.07	4.13
W	0.70	1.38	0.64	0.76	0.85	1.05	0.90	1.42	1.06	1.04	0.49	0.71
Re	0.00	0.00	0.00	0.00	0.00	0.00	0.00	0.00	0.00	0.00	0.00	0.00
Tl	0.04	0.04	0.04	0.04	0.04	0.04	0.04	0.04	0.04	0.04	0.07	0.09
Pb	3.08	3.12	2.69	2.98	2.83	2.88	2.74	3.07	3.70	2.98	5.45	5.70
Bi	0.01	0.00	0.00	0.00	0.00	0.00	0.00	0.00	0.00	0.00	0.02	0.01
Th	7.02	7.42	6.54	7.14	6.75	6.98	6.56	7.18	7.22	7.24	10.90	12.50
U	1.33	1.40	1.23	1.35	1.26	1.32	1.22	1.35	1.38	1.36	2.10	2.56
Zr	296	315	288	308	301	304	290	312	317	317	406	422
Hf	6.32	6.27	5.94	6.29	5.84	6.08	5.94	6.31	6.51	6.26	7.76	8.25
Eu*	1.02	1.05	1.01	1.01	1.03	1.00	1.01	1.02	1.01	1.01	1.01	0.99
$(La/Yb)_N$	18.23	20.46	18.69	19.57	19.70	19.63	19.12	19.61	19.25	19.83	33.23	30.43
∑REE	210.56	220.51	201.20	217.26	207.41	211.20	203.02	218.91	221.29	217.79	314.10	332.08
∑HREE	18.79	18.03	17.75	18.45	16.83	17.80	17.51	18.59	18.99	18.39	20.93	22.58
∑LREE	191.77	202.48	183.45	198.81	190.58	193.40	185.51	200.32	202.30	199.40	293.17	309.50
∑LREE/∑HREE	10.21	11.23	10.34	10.78	11.32	10.87	10.60	10.78	10.65	10.85	14.01	13.71
$(La/Sm)_N$	3.82	4.27	3.97	4.11	4.26	4.11	3.99	4.11	4.09	4.12	4.46	4.41
$(Gd/Yb)_N$	3.13	3.09	3.14	3.13	2.88	3.08	3.09	3.11	3.11	3.16	4.51	4.13

*Fe_2O_{3T} = FeO*1.1113 + Fe_2O_{3T} in wt.%; ∑REE = total REE concentration; ∑LREE = total LREE concentration; ∑HREE = total HREE concentration; subscript N denotes normalization to the chondrite value of Sun and McDonough (1989); Eu* = $Eu_N/(Sm_N + Gd_N)^{1/2}$.*

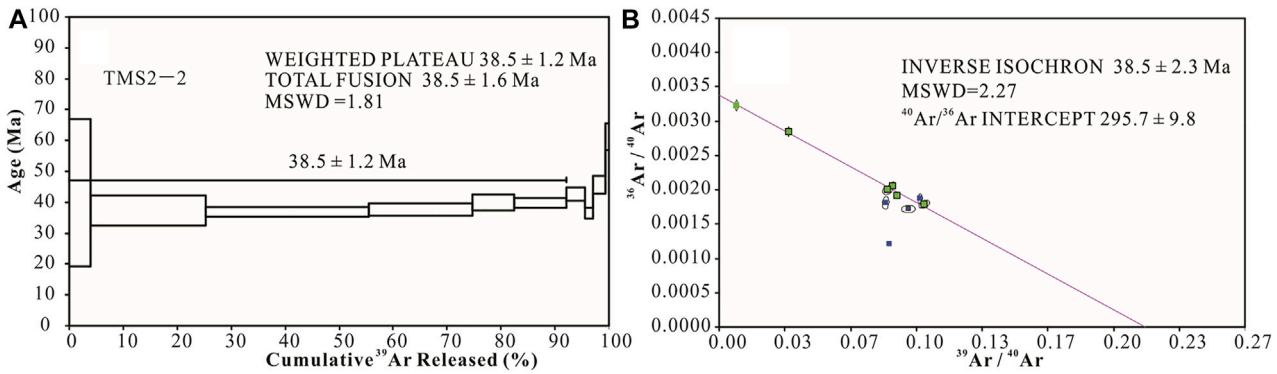

FIGURE 5 | Plateau and isochron Ar–Ar ages for sample TMS2-2. **(A)** and isochron Ar-Ar age **(B)** for sample TMS2-2.

precision of ~0.002%. Measured $^{143}Nd/^{144}Nd$ ratios were normalized to a $^{146}Nd/^{144}Nd$ value of 0.7219, and analysis of the La Jolla Nd standard yielded a measured $^{143}Nd/^{144}Nd$ ratio of 0.511851 ± 45. Single-stage Nd model ages (T_{DM1}) are calculated relative to the depleted mantle reservoir (Depaolo, 1988), and two-stage Nd model ages (T_{DM2}) are calculated for different ages of magmatism relative to average continental crustal values with a $^{147}Sm/^{144}Nd$ ratio of 0.118 (Jahn and Condie, 1995).

4 ANALYTICAL RESULTS

4.1 Ar–Ar Geochronology

The Funding basalt samples (TMS2-2 and TMS2-1) from the Fotan volcanic succession dated by the $^{40}Ar/^{39}Ar$ method yielded apparent ages that were determined using age spectra and isotope correlation ($^{36}Ar/^{40}Ar$ vs. $^{39}Ar/^{40}Ar$) diagrams (**Figures 5**, **6**; **Tables 1**,**2**). The latter provides a quantitative measure of the initial argon composition and allows the identification of excess argon that has $^{40}Ar/^{36}Ar$ ratios greater than the present day atmospheric value of 295.5. The data in **Table 1** and **Figure 2** indicate that little excess argon was present in the basalt samples.

The plateau age for sample TMS2-2 is 38.5 ± 1.2 Ma (**Figure 5A**), a date that is within error of the isochron age for this sample (38.5 ± 2.3 Ma; **Figure 5B**). The second sample (TMS2-1) was collected from the basal section of the Fuding area and yielded an older plateau age (42.3 ± 2 Ma; **Figure 6**). As such, we interpret the plateau ages for these samples to represent the volcanism that formed the Fuding basalts, indicating that the final eruption of the Fotan Formation occurred at 42.3–38.5 Ma. Hence, the eruption of the Fuding basalt occurred at 42.3–38.5 Ma, during the Eocene.

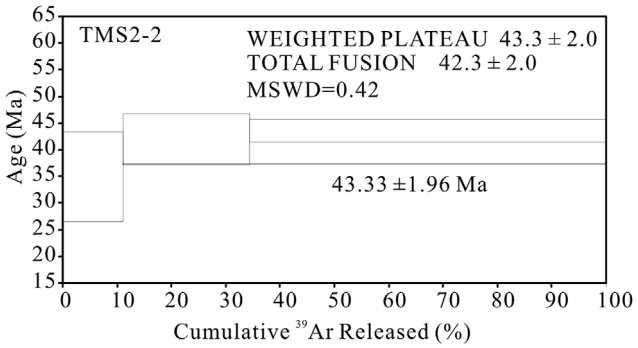

FIGURE 6 | Plateau Ar–Ar age for sample TMS2-1.

4.2 Whole-Rock Geochemical Characteristics

4.2.1 Gabbro and Diabase

The gabbro and diabase samples from the Fuding area have restricted ranges of SiO_2 (46.54–47.03 wt.%), total Fe expressed as FeO (FeO_T; 11.34–12.32 wt.%), CaO (8.92–10.07 wt.%), and Al_2O_3 (12.12–14.23 wt.%) concentrations, but a wide range of MgO concentrations (8.64–10.17 wt.%). Plotting these samples on a total alkali versus silica (TAS; SiO_2 versus $Na_2O + K_2O$) classification diagram indicates the majority are trachybasalts with a few basalts, although all of the samples plot above the alkaline curve in this diagram (**Figure 7A**). These samples have K_2O and $K_2O + Na_2O$ concentrations of 1.99–2.35 and 4.67–5.65 wt.%, respectively, yielding high K_2O/Na_2O ratios (0.65–0.82) that indicate these samples are alkaline basaltic rocks (**Figures 7B,C,D**).

Plotting data of the gabbro and diabase samples on Harker diagrams yields negative correlations between SiO_2 and CaO, FeOT, and MgO concentrations, and positive correlations between SiO_2 and Na_2O, K_2O, and Al_2O_3 concentrations (**Figure 8**).

All of the gabbro and diabase samples have high total REE (ΣREE) values (201.2–221.29 ppm; average of 212.91 ppm) and they are light REE (LREE) enriched, with total LREE to total heavy REE (HREE; ΣLREE/ΣHREE) ratios of 10.21–11.32 (average of 10.76). These samples have $(La/Yb)_N$ (where $_N$ denotes normalization to the chondrite ratio of Sun and McDonough, 1989) ratios of 18.26–20.46 (average of 19.41), reflecting the degree of fractionation of the LREE from the

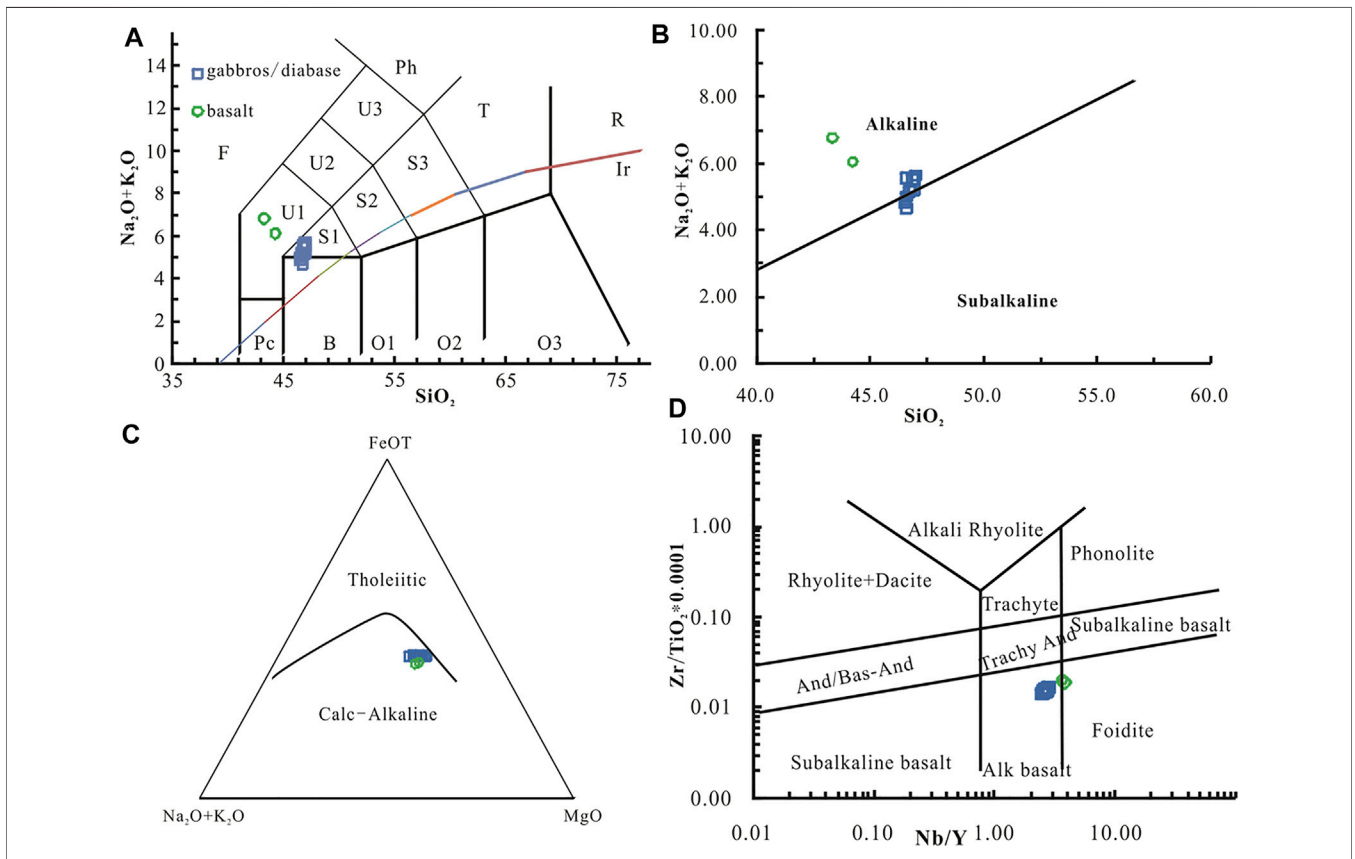

FIGURE 7 | Geochemical classification diagrams showing variations in the compositions of samples from the Fuding mafic volcanic neck. **(A)** Total alkali versus silica (TAS) diagram (after Middlemost, 1994); **(B)** SiO_2 vs. $K_2O + Na_2O$ diagram (after LeMaitre et al., 1989); **(C)** AFM diagram; and **(D)** Zr/TiO_2 versus Nb/Y diagram (after Pearce, 1996).

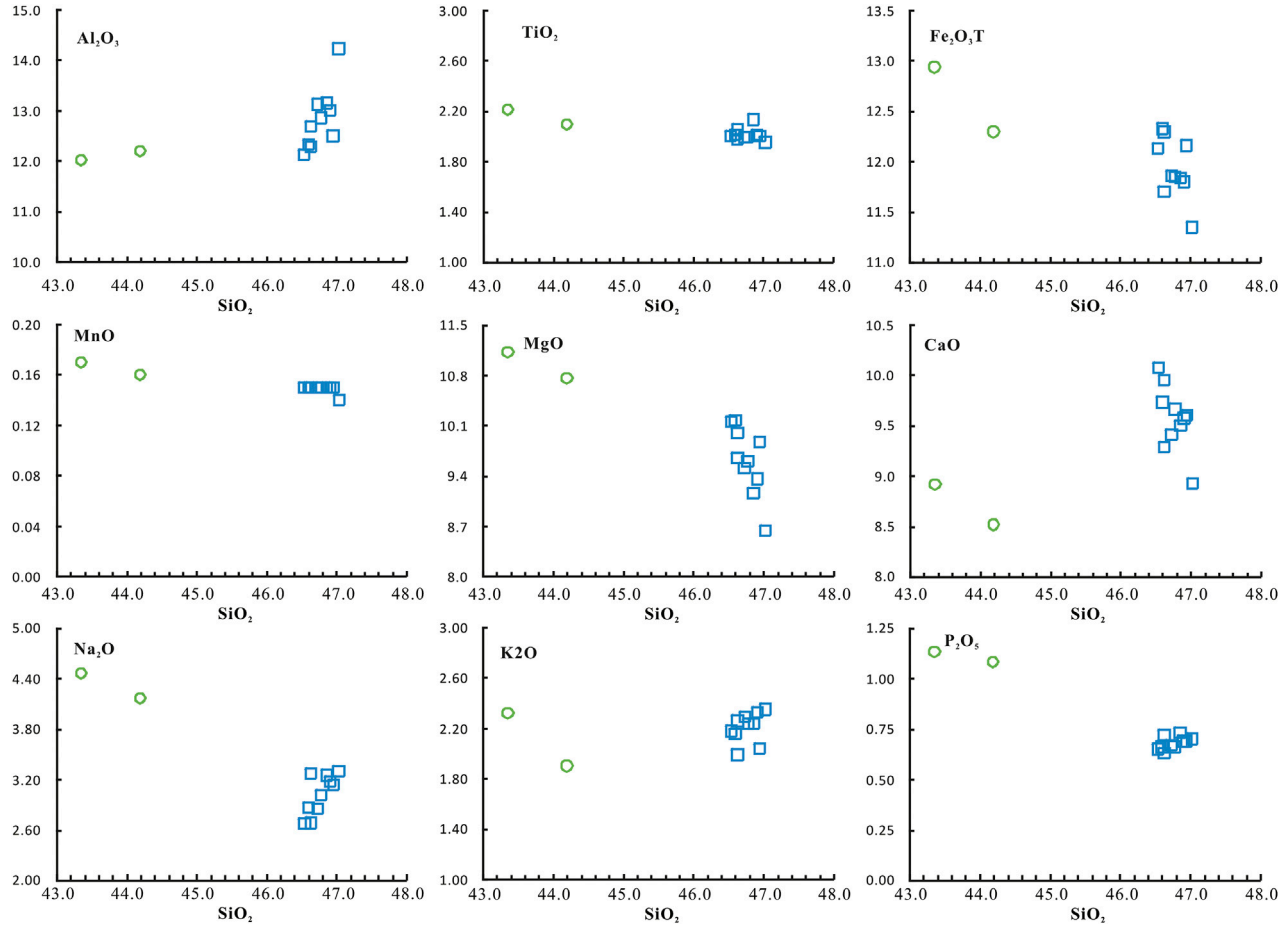

FIGURE 8 | Harker-type diagrams showing variations in the geochemical compositions of mafic rocks from the Fuding volcanic neck.

HREE. These samples show $(La/Sm)_N$ values from 3.82 to 4.27 (average of 4.09) and $(Gd/Yb)_N$ values from 2.88 to 3.16 (average of 3.09). They are free of significant Eu anomalies ($Eu/Eu^* = 1.00–1.05$, average of 1.02) and have smooth chondrite-normalized REE patterns (**Figure 9A**). All of the samples are enriched in the large ion lithophile elements (LILE), have differentiated high field strength element (HFSE) concentrations, and are slightly depleted in Ti and Y (**Figure 9C**). They have chondrite-normalized REE and primitive-mantle-normalized multi-element variation patterns that are similar to those of typical OIB compositions but differ from typical N- or E-type mid-ocean-ridge basalt (MORB) compositions.

4.2.2 Basalts

The basalts analyzed during this study contain higher concentrations of MgO (10.75–11.12 wt.%) than the gabbro and diabase samples, with both basalt samples classified as tephrites or basanites and both plotting above the alkaline curve (**Figure 7A**), indicating that both of these basalts are alkaline basaltic rocks (**Figures 7B,D**).

Both of the basalt samples contain higher ΣREE concentrations (314.10–332.08 ppm; average of 323.09 ppm) than the gabbro and diabase samples, although the basalts are similar to these other samples in that they have OIB-type REE and multi-element variation diagram characteristics that contrast with typical N- or E-type MORB compositions (**Figures 9B,D**).

4.3 Whole-Rock Sr–Nd Characteristics

The isotopic Rb–Sr and Sm–Nd ratios of the whole-rock samples are given in **Table 4**. The gabbro, diabase, and basalt samples have uniform initial εNd(t) (3.05–4.56, average of 3.90) and initial $^{87}Sr/^{86}Sr$ (0.703794–0.703911, average of 0.703865) values. They have two-stage Nd model (T_{DM2}) ages than range from 0.61 to 0.73 Ga (average of 0.67 Ga).

5 DISCUSSION

5.1 Petrogenetic Evolution

5.1.1 Basalts

The basalts from the Fuding mafic volcanic neck are enriched in the REE and have highly differentiated HFSE compositions that are apparent in their OIB-type primitive-mantle-normalized multi-element diagrams (**Figures 9B,D**; Edwards et al., 1994;

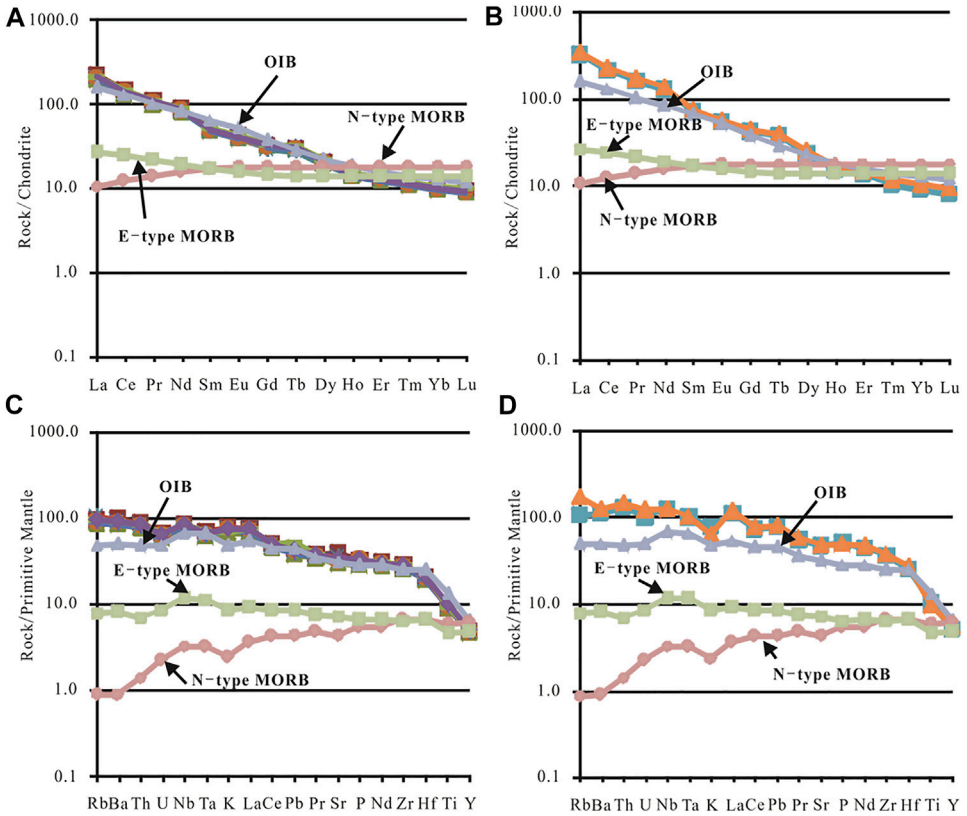

FIGURE 9 | Chondrite-normalized REE and primitive-mantle-normalized multi-element diagrams for samples from the Fuding mafic volcanic neck. Diagrams are normalized to the chondrite and primitive mantle compositions of Sun and McDonough (1989). **(A)** and **(C)** for gabbro and diabase samples; **(B)** and **(D)** for basalt samples.

TABLE 4 | Rb–Sr and Sm–Nd isotopic compositions of mafic volcanics from the northeast of Northeast Fujian Province.

Sample	Rock types	Age (Ma)	Rb (ppm)	Sr (ppm)	$^{87}Rb/^{86}Sr$	$^{87}Sr/^{86}Sr$	I_{Sr}	Sm (ppm)	Nd (ppm)	$^{147}Sm/^{144}Nd$	$^{143}Nd/^{144}Nd$	εNd	t_{Nd} (Ga)
TMS-1-1	Gabbro/ Diabase	38.5	59.0	691	0.247	0.704 016 ± 7	0.703 881	7.83	40.4	0.117 2	0.512 808 ± 11	3.71	0.68
TMS-1-2		38.5	60.0	833	0.208	0.704 025 ± 6	0.703 911	7.65	40.9	0.113 1	0.512 817 ± 12	3.90	0.67
TMS-1-4		38.5	55.0	627	0.254	0.704 016 ± 5	0.703 878	7.34	38	0.116 8	0.512 774 ± 9	3.05	0.73
TMS-2-5		38.5	66.0	739	0.258	0.704 018 ± 5	0.703 877	7.79	41.1	0.114 6	0.512 783 ± 9	3.23	0.72
TMS-2-6		38.5	60.0	692	0.251	0.704 006 ± 6	0.703 868	7.86	41.6	0.114 2	0.512 851 ± 8	4.56	0.61
TMS-3-1		38.5	59.0	694	0.246	0.703 997 ± 6	0.703 862	7.72	40.8	0.114 4	0.512 849 ± 9	4.52	0.62
TMS-2-1	Basalt	42.3	107	991	0.312	0.703 982 ± 5	0.703,794	11.4	62.9	0.109 6	0.512 843 ± 8	4.47	0.62
TMS-2-2		42.3	58.0	652	0.257	0.704 006 ± 7	0.703 851	7.53	39.5	0.115 3	0.512 808 ± 10	3.76	0.68

Sun and McDonough, 1989; Zhao and Zhou, 2007). Both of these samples are classified as within-plate alkali basalts in the Nb–Zr–Y diagram of Meschede ,1986; **Figure 10A**). These basalts have Ti/V ratios between 75 and 80 that are much higher than those of arc basalts, and they plot in the OIB field on a modified Ti versus V diagram (**Figure 10B**; Shervais, 1982). Both samples plot in the OIB field on a Nb/Yb versus Th/Yb diagram (**Figure 10C**; J. Pearce and Peate, 1995). They yield high Mg# values (= 100*MgO/(MgO + 0.85*Fe_2O_3T) and contain low concentrations of SiO_2, suggesting that they originated from a

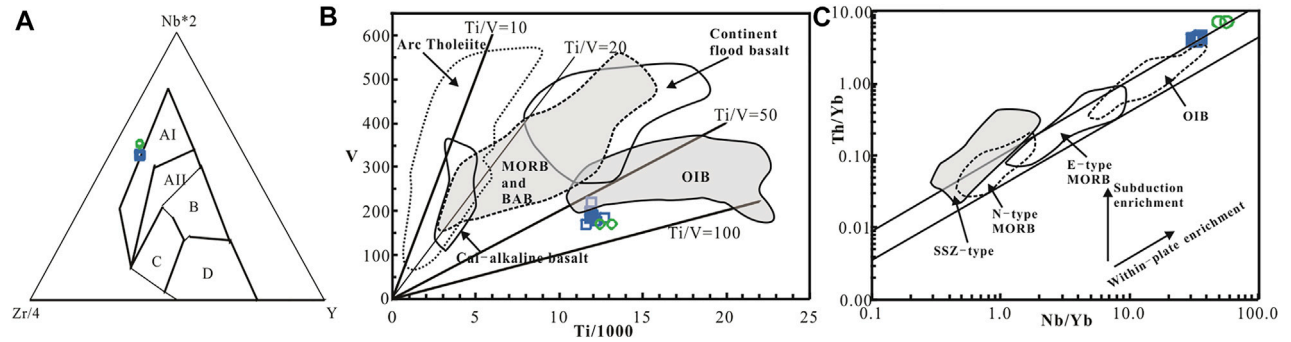

FIGURE 10 | (A) Nb-Zr-Y, **(B)** Ti versus V (after Shervais, 1982) and **(C)** Th/Yb–Nb/Yb (after Pearce & Peate, 1995) diagrams for samples from the study area. Average N-MORB, E-MORB, and OIB compositions are from Sun and McDonough (1989), and SSZ-, N-MORB-, E-MORB-, and OIB-type fields are from Mahe et al., 2004, Saccani and Photiades (2005), and Aldanmaz et al., 2008.

parental magma that was derived from an OIB-like mantle source in a continental rift environment, without any crustal input.

5.1.2 Gabbro and Diabase

The gabbro and diabase samples from the Fuding area have similar REE and HFSE characteristics as the basalt samples, again indicating that these units have an OIB-type affinity (**Figures 9A,C**, **Figures 10A–C**; Edwards et al., 1994; Sun and McDonough, 1989; Zhao and Zhou, 2007). However, the gabbro and diabase units have Mg# values of 63.96–66.58, suggesting that they record the minor differentiation of olivine and pyroxene. This fractionation is also evidenced by a negative

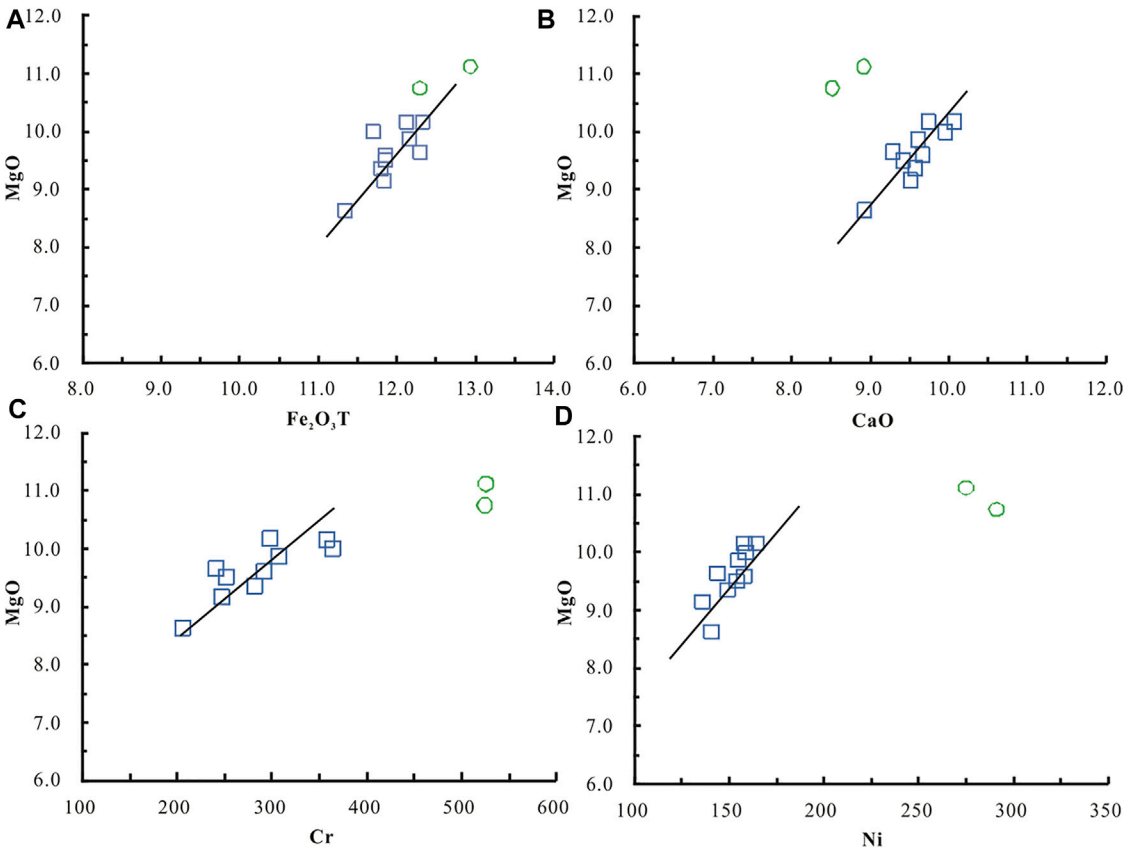

FIGURE 11 | Harker-type diagrams showing variations in the Fe_2O_3T, CaO, Cr, and Ni concentrations of samples from the Fuding area relative to MgO. **(A)**, CaO **(B)**, Cr **(C)**, and Ni **(D)** concentrations of samples from the Fuding area relative to MgO.

correlation between SiO_2 and MgO concentrations (**Figure 8**). In addition, the positive correlation between Fe_2O_3T and MgO concentrations shown by the gabbro samples is indicative of the fractionation of olivine (**Figure 11A**), whereas the positive correlation between CaO and MgO concentrations in these samples is evidence of the fractionation of clinopyroxene (**Figure 11B**). This conclusion is also supported by the presence of positive correlations between Cr, Ni, and MgO concentrations (**Figures 11C,D**).

The lack of any significant Eu anomalies (Eu/Eu* = 1.00–1.05; **Figure 9A**) indicates that the gabbro and diabase units do not record any plagioclase fractionation. However, crustal contamination can modify the composition of mantle-derived magmatic rocks. Crustal materials are enriched in the LILE, K_2O, and Na_2O, and are depleted in P_2O_5 and TiO_2. The gabbro and diabase units within the Fuding area contain low and invariant concentrations of K_2O and Na_2O, suggesting that they record minimal amounts of crustal contamination. Crustal contamination can also produce negative Nb and Ta, and positive Zr and Hf anomalies relative to the LILE and LREE (Sun and McDonough, 1989; Zhao and Zhou, 2007); however, these anomalies are absent in the primitive-mantle-normalized multi-element diagrams for the gabbro and diabase samples from the study area (**Figure 9C**), again suggesting that these units record minimal crustal contamination. All of the samples show low initial $^{87}Sr/^{86}Sr$ values (average of 0.703865) and high εNd(t) values (3.05–4.56, average of 3.90). These data indicate that the basalt, gabbro, and diabase units in the Fuding area were derived from an OIB-type mantle source, with the gabbro and diabase units recording minor amounts of crustal contamination.

5.2 Implications of Ar–Ar Dating

The basalts from the Fuding mafic volcanic neck in coastal SE China are generally alkaline (average $Na_2O + K_2O$ = 5.77 wt.%) and are enriched in TiO_2 (average TiO_2 = 2.15 wt.%), whereas Neogene basalts in this area are largely subalkaline (average $Na_2O + K_2O$ = 2.79 wt.%) and contain lower concentrations of TiO_2 (average $TiO_{2=}$<1.5 wt.%; Lu et al., 2000), indicating significant geochemical differences between these basalts.

The trace and REE compositions of the Fuding mafic volcanic neck are different from those of the Neogene basalts of coastal SE China. The basalts from the former contain higher Rb (average of 87 ppm), Sr (average of 984 ppm), Ba (average of 807 ppm), and total REE (average of 243 ppm) concentrations and have higher light REE/heavy REE (LREE/HREE) ratios (average of 11.93) than the Neogene basalts of coastal SE China (average Rb, Sr, Ba, and total REE concentrations of 17.5, 339, 201, and 112 ppm, respectively, with an average LREE/HREE ratio of 4.22; Lu et al., 2000; J. Qiu et al., 1999; S. Wang, 1998; X. Wang et al., 2012; J. Zhang and Lu, 1997; Zouet al, 2000).

L. Li et al. (2011) reported that the Taimushan granite formed at 96.16 ± 1.6 Ma and suggested that the Fuding basalts formed part of the late Oligocene to middle Pleistocene Fotan Group. Our unpublished zircon U–Pb laser ablation (LA)–ICP–MS analyses yielded a Late Cretaceous age of 88.2 ± 1.0 Ma for these basalts, although these ages may be unreliable. The two basalt samples from the Fuding mafic volcanic neck yield similar Ar–Ar ages of 38.5 ± 1.2 and 42.3 ± 2 Ma, indicating that the basalts within both the neck and within the Fotan Group were emplaced during the Eocene.

5.3 Implications of the Presence of Peridotite Xenoliths

Cretaceous basalts in coastal SE China are usually associated with other contemporaneous bimodal volcanic rocks. The basalts in this area crop out over a much smaller area than associated acidic volcanic rocks and are thought to have been derived from either an enriched region of mantle, from a depleted region of the mantle and then either assimilated crustal material or underwent magma mixing, or were derived from the crust–mantle transition zone (C. Chen et al., 2008; Cui et al., 2011; He and Xu, 2011; Z. Li and Li, 2007; X. Li et al., 2007; H. Li et al., 1995; Tang et al., 2010; Xing et al., 1999; G. Xie et al., 2005; X. Xu et al., 2008; J. Yan et al., 2005b; Yu et al., 1993).

As mentioned above, both the petrogenesis of the basalts in coastal SE China and the nature of the mantle beneath this region remain uncertain. The main cause of this uncertainty is the lack of mantle rocks in this area; however, peridotite xenoliths within the Fuding basalts can be used to determine the characteristics of the Eocene mantle in this area, including the post late-Mesozoic evolution of the mantle beneath coastal SE China.

The nature of the late Mesozoic mantle in coastal SE China remains debated. Several different models have been proposed, including 1) enriched lithospheric mantle beneath Fujian and Zhenjiang provinces (Cui et al., 2011; Tang et al., 2010; G. ; Xie et al., 2005; J. ; Yan et al., 2003; J. ; Yan et al., 2005a; Yan et al., 2005b; Z. ; Yang et al., 1999; B. ; Zhang et al., 2004), 2) enriched mantle that mixed with both depleted and EMII type enriched mantle material (X. Xie et al., 2001), 3) local areas of weakly enriched mantle that is compositionally similar to EMII-type enriched mantle (H. Zhang et al., 2005), and 4) depleted asthenospheric mantle (Q. Zhou et al., 2010).

Both the late Mesozoic basalts and acidic volcanic rocks in coastal SE China have isotopic characteristics similar to those of enriched mantle (C. Dong C. W. et al., 2006; Y. Dong Y. X. et al., 2006; C. Dong et al., 2007; Z. Yang et al., 1999; Xing et al., 1999; Xue et al., 1996; J. Zhou and Chen, 2001), suggesting that the Cretaceous upper mantle in this region was relatively stable but also weakly enriched.

The Paleocene basalts in coastal SE China generally crop out in the northern parts of the Jiangsu and Hefei basins, as well as in the Mingguang and Fushan areas (Qian and Li, 1996; Z. ; Yang et al., 1999). These basalts contain abundant peridotite xenoliths, were emplaced at 64–56 Ma, have the characteristics of typical continental basalts, and were derived from weakly enriched mantle (D. Chen, 1992; Cong et al., 1996; Z. Yang et al., 1999; X. Zhou, 1992).

Eocene basalts are sporadically exposed within coastal SE China and have been reported from the Sanshui Basin in Guangdong Province (Y. Dong Y. X. et al., 2006; Hu et al., 2013; Xiao et al., 2006; X. Zhang et al., 1993; W. Zhang and Fang, 2014; Zhu et al., 1991). X. Zhang et al. (1993) reported

K–Ar ages of 45–55 Ma for these basalts, and Y. Dong Y. X. et al. (2006) obtained a zircon U–Pb age of 46–45 Ma for basaltic rocks in the Sanshui Basin. The latter basalts are thought to have been generated by partial melting of a depleted region of the mantle that generated continental rift-type magmatic rocks (Y. Dong Y. X. et al., 2006; W. Zhang and Fang, 2014), or partial melting of an enriched region of the mantle within a continental rift setting (Hu et al., 2013). The Sanshui basalts yield recalculated εNd(t) values of −0.77 to +1.23 (mean age 50 Ma) (Zhu et al., 1991) that reflect the weakly depleted nature of the Eocene mantle in coastal SE China. The basalt, gabbro, and diabase units within the Fuding area have OIB-type geochemical affinities with low initial $^{87}Sr/^{86}Sr$ ratios (average of 0.703865) and high εNd(t) values (average of 3.90) which similar with the depleted mantle. Its OIB type geochemical characteristics may be inherited from crustal materials with similar characteristics. Meanwhile, the widespread Neogene basalts in coastal SE China are exposed in the Xinchang area of Zhejiang Province, the Jiashan area of Anhui province, the Fangshan area of Jiangsu province, and the Sanshui Basin in Guangdong Province, and all of these Neogene basalts were derived from a depleted region of the mantle (R. Wang and Yang, 1987a, Wang and Yang, 1987b; Zhi et al., 1994). Thus, the mantle beneath coastal SE China evolved between the Cretaceous and the Neogene from enriched to depleted, and this change occurred during the Eocene.

6 CONCLUSION

Whole-rock Ar–Ar analyses of two basalt samples from the Fuding mafic volcanic neck yield ages of 38.5 ± 1.2 and 42.3 ± 2 Ma, indicating that the basalts were erupted at 42.3–38.5 Ma.

The basalt, gabbro, and diabase units within the Fuding area have OIB-type geochemical affinities with low initial $^{87}Sr/^{86}Sr$ ratios (average of 0.703865) and high εNd(t) values (average of 3.90). Both gabbro and diabase units record minor amounts of crustal contamination.

Peridotite xenoliths within the Fuding basalt provide evidence of the nature of the Eocene mantle in this area, especially the post late-Mesozoic evolution of the mantle beneath coastal SE China. The mantle beneath coastal SE China evolved from enriched to depleted between the Cretaceous and the Neogene, with this change occurring during the Eocene.

DATA AVAILABILITY STATEMENT

The original contributions presented in the study are included in the article/supplementary material, further inquiries can be directed to the corresponding author.

AUTHOR CONTRIBUTIONS

XZ designed the study. CL wrote the first draft. YJ analyzed the geochemical data. GX drew some of the figures. MY and ZD completed the geochemical experimental analysis. All authors discussed the results and contributed to the preparation of the manuscript.

FUNDING

This work was supported by Geological Survey projects (DD20221633) of the China Geological Survey, National key research and development program (No 2016YFC0600205) and Geological Survey projects (Nos 121201008000150002, 1212011121098, 121201008000150002, and 12120113070800) of the China Geological Survey.

REFERENCES

Aldanmaz, E., Yaliniz, M. K., Güctekin, A., and Göncüoğlu, M. C. (2008). Geochemical Characteristics of Mafic Lavas from the Neotethyan Ophiolites in Western Turkey: Implications for Heterogeneous Source Contribution during Variable Stages of Ocean Crust Generation. *Geol. Mag.* 145, 37–54. doi:10.1017/s0016756807003986

Bodinier, J.-L., Garrido, C. J., Chanefo, I., Bruguier, O., and Gervilla, F. (2008). Origin of Pyroxenite-Peridotite Veined Mantle by Refertilization Reactions: Evidence from the Ronda Peridotite (Southern Spain). *J. Petrology* 49, 999–1025. doi:10.1093/petrology/egn014

Chen, C.-H., Lee, C.-Y., Lu, H.-Y., and Hsieh, P.-S. (2008). Generation of Late Cretaceous Silicic Rocks in SE China: Age, Major Element and Numerical Simulation Constraints. *J. Asian earth Sci.* 31, 479–498. doi:10.1016/j.jseaes.2007.08.002

Chen, D. G. (1992). "Geochemistry of Cenozoic Basalts in the Southern Section of Tanlu Fault," in *Geochemistry of Cenozoic Volcanic Rocks of China*. Editor R. X. LIU (Beijing: Earthquake press), 171–209. (in Chinese).

Chen, D. G., Xia, Q. K., and Zhi, X. C. (1997). Geochemistry of Megacrysts in Cenozoic Basalts of Eastern China. *Acta Geosci. Sin.* 18, 299–306. (in Chinese with English abstract).

Cong, B. L., Wang, Q. C., Zhang, H. Z., Yan, X., and Jiang, L. L. (1996). Petrogenesis of Cenozoic Volcanic Rocks in Hefei Basin, China. *Acta Petrol. Sin.* 3, 370–381. (in Chinese with English abstract).

Cui, Y. R., Xie, Z., Wang, B., Chen, J. F., Yu, Y. W., and He, J. F. (2011). Geochemical Characteristics of the Late Mesozoic Basalts in Southeastern Zhejiang Province and Constraints on Magma Source Materials. *Geol. J. China Univ.* 17, 492–512. (in Chinese with English abstract). doi:10.1007/s11769-011-0446-4

Dai, Q. Z., and Chen, R. K. (2008). On the Geologic Characteristics and Formation Mechanisms of the Basalt Pillars in Shanhoujian, Fuding City. *Geol. Fujian* 4, 369–377. (in Chinese with English abstract).

Deng, J. F., E, M. L., and Lu, F. X. (1988). The Chemistry of Hannuoba Basalts and Their Trends of Magmatic Revolution. *Acta Petrol. Sin.* 4, 22–33. (in Chinese with English abstract).

Depaolo, D. J. (1988). *Neodymium Isotope Geochemistry: An Introduction*. New York: Springer-Verlag, 181.

Dong, C. W., Xu, X. S., Chen, X. M., and Zhou, X. M. (1997). Mineralogical Record of Crystallization Processes of Pingtan Hornblende Gabbro, Fujian. *Acta Mineral. Sin.* 17, 285–290. (in Chinese with English abstract).

Dong, C. W., Xu, X. S., Yan, Q., Lin, X. B., and Zhu, G. Q. (2007). A New Case of Late Mesozoic Crust-Mantle Interaction in Eastern Zhejiang: Geochronology and Geochemistry of the Ru'ao Diabase-Granite Composite Intrusions. *Acta Petrol. Sin.* 23, 1303–1312. (in Chinese with English abstract). doi:10.3969/j.issn.1000-0569.2007.06.007

Dong, C. W., Zhang, D. R., Xu, X. S., Yan, Q., and Zhu, G. Q. (2006a). SHRIMP U-Pb Dating and Litho Geochemistry of Basic-Intermediate Dike Swarms

from Jinjiang, Fujian Province. *Acta Petrol. Sin.* 22, 1696–1702. (in Chinese with English abstract). doi:10.1016/j.sedgeo.2006.03.014

Dong, Y. X., Xiao, L., Zhou, H. M., Zeng, G. C., Wang, X. D., Xiang, H., et al. (2006b). Spatial Distribution and Petrological Characteristics of the Bimodal Volcanic Rocks from Sanshui Basin, Guangdong Province: Implication for Basin Dynamics. *Geotect. Metallogenia* 30, 82–92. (in Chinese with English abstract). doi:10.3969/j.issn.1001-1552.2006.01.010

Dong, Z. X., Chen, L. H., Yang, J. M., and Ma, H. W. (1999). The Characteristics of Spinel Compositions in Mantle-Derived Xenoliths from Alkali Basalts and Their Petrogenetic Significance. *Acta Petrol. Sin.* 15, 607–615. (in Chinese with English abstract).

Edwards, C. M. H., Menzies, M. A., Thirlwall, M. F., Morris, J. D., Leeman, W. P., and Harmon, R. S. (1994). The Transition to Potassic Alkaline Volcanism in Island Arcs: The Ringgit--Beser Complex, East Java, Indonesia. *J. Petrology* 35, 1557–1595. doi:10.1093/petrology/35.6.1557

Guo, F., Guo, J. T., Wang, Y., Fan, W. M., Li, C. W., Li, H. X., et al. (2013b). The Genesis of Lower $\delta^{18}O$ Olivine Basalts in Junan and Qingdao Area, Jiangsu-Shangdong Provinces. *Sci. China* 58, 1289–1299. doi:10.1007/s11434-012-5607-z

Guo, F., Guo, J., Wang, Y., Fan, W., Li, C., Li, H., et al. (2013a). A Metasomatized Mantle Wedge Origin for Low-δ 18O Olivine in Late Cretaceous Junan and Qingdao Basalts in the Sulu Orogen. *Chin. Sci. Bull.* 58, 3903–3913. doi:10.1007/s11434-012-5607-z

He, Z. Y., and Xu, X. S. (2011). Petrogenesis of the Late Yanshanian Mantle-Derived Intrusions in Southeastern China: Response to the Geodynamics of Paleo-Pacific Plate Subduction. *Chem. Geol.* 328, 208–221.

Hu, J. J., Li, Q., Zhai, Y. J., Zhang, W., Zhang, Y. F., and Bai, X. Y. (2013). Distribution and Geodynamics of Volcanic Rock of the Huayong Group, Sanshui Basin, Guangdong Province. *J. East China Inst. Technol. Sci.* 36, 175–181. (in Chinese with English abstract). doi:10.3969/j.issn.1674-3504.2013.02.011

Jahn, B.-M., and Condie, K. C. (1995). Evolution of the Kaapvaal Craton as Viewed from Geochemical and SmōNd Isotopic Analyses of Intracratonic Pelites. *Geochimica Cosmochimica Acta* 59, 2239–2258. doi:10.1016/0016-7037(95)00103-7

Koppers, A. A. P. (2002). ArArCALC-software for 40Ar/39Ar Age Calculations. *Comput. Geosciences* 28, 605–619. doi:10.1016/s0098-3004(01)00095-4

LeMaitre, R. W., Bateman, P., Dudek, A., Keller, J., Lebas, M. J. L., Sabine, P. A., et al. (1989). *A Classication of Igneous Rocks and Glossary of Terms*. Oxford: Blackwell.

Li, H. M., Dong, C. W., Xu, X. S., and Zhou, X. M. (1995). Single Grain Zircon U-Pb Dating of Quanzhou Gabbro: Origin of the Mafic Magmativte in the Southeast Fujian Province. *Chin. Sci. Bull.* 40, 158–160. (in Chinese with English abstract).

Li, L. L., Zhou, H. W., Chen, Z. H., Wang, J. R., and Xiao, Y. (2011). Geochemical Characteristics of Granites in Taimushan Area, Fujian Province, and Their Geological Significance. *Acta Petrologica Mineralogica* 30, 593–609. (in Chinese with English abstract). doi:10.1007/s11589-011-0776-4

Li, T. F., and Ma, H. W. (2002). Clinopyroxene-melt Equilibrium Temperature and Pressure of Cenozoic Basalts with Special Reference to the Genesis of Mantle Xenoliths in Some Areas of Eastern China. *Acta Petrologica Mineralogica* 21, 11–23. (in Chinese with English abstract).

Li, X.-h. (2000). Cretaceous Magmatism and Lithospheric Extension in Southeast China. *J. Asian Earth Sci.* 18, 293–305. doi:10.1016/s1367-9120(99)00060-7

Li, X.-H., Li, Z.-X., Li, W.-X., Liu, Y., Yuan, C., Wei, G., et al. (2007). U-pb Zircon, Geochemical and Sr-Nd-Hf Isotopic Constraints on Age and Origin of Jurassic I- and A-type Granites from Central Guangdong, SE China: A Major Igneous Event in Response to Foundering of a Subducted Flat-Slab? *Lithos* 96, 186–204. doi:10.1016/j.lithos.2006.09.018

Li, Z.-X., and Li, X.-H. (2007). Formation of the 1300-km-wide Intracontinental Orogen and Postorogenic Magmatic Province in Mesozoic South China: A Flat-Slab Subduction Model. *Geol* 35, 179–182. doi:10.1130/g23193a.1

Liu, C. Q., Xie, G. H., and Akimasa, M. (1995). Geochemistry of Cenozoic Basalts from Eastern China--I. Major Element and Trace Element Compositions: Petrogenesis and Characteristics of Mantle Source. *Geochimica* 24, 1–19. (in Chinese with English abstract). doi:10.1016/S1872-5813(08)60001-8

Liu, J. H., and Yan, J. (2007). Peridotitic Xenoliths in the Cenozoic Basalts from the Subei Basin. *Mineral. Pet.* 27, 39–46. (in Chinese with English abstract).

Lu, Q. D., Zhu, G. L., and Qing, Z. J. (2000). Geochemical Feature and Genesis of the Mesozoic and Cenozoic Basalt in Fujian Province. *Regional Geol. China* 19, 85–91. (in Chinese with English abstract).

Mahéo, G., Bertrand, H., Guillot, S., Villa, I. M., Keller, F., and Capiez, P. (2004). The South Ladakh Ophiolites (NW Himalaya, India): an Intra-oceanic Tholeiitic Arc Origin with Implication for the Closure of the Neo-Tethys. *Chem. Geol.* 203, 273–303. doi:10.1016/j.chemgeo.2003.10.007

Meschede, M. (1986). A Method of Discriminating between Different Types of Mid-ocean Ridge Basalts and Continental Tholeiites with the Nbō1bZrō1bY Diagram. *Chem. Geol.* 56, 207–218. doi:10.1016/0009-2541(86)90004-5

Middlemost, E. A. K. (1994). Naming Materials in the Magma/igneous Rock System. *Earth-Science Rev.* 37, 215–224. doi:10.1016/0012-8252(94)90029-9

Pearce, J. A. (1996). "A User's Guide to Basalt Discrimination Diagrams," in *Trace Element Geochemistry of Volcanic Rocks: Applications for Massive Sulfide Exploration*. Editor D. A. Wyman (St. John's,Canada: Geological Association of Canada), 12, 79–113.

Pearce, J. A., and Peate, D. W. (1995). Tectonic Implications of the Composition of Volcanic Arc Magmas. *Annu. Rev. Earth Planet. Sci.* 23, 251–285. doi:10.1146/annurev.ea.23.050195.001343

Pei, F. P., Xu, W. L., Wang, Q. H., Wang, D. Y., and Lin, J. Q. (2004). Mesozoic Basalt and Mineral Chemistry of the Mantle-Derived Xenocrysts in Feixian, Western Shandong, China: Constraints on Nature of Mesozoic Lithospheric Mantle. *Geol. J. China Univ.* 10, 88–97. (in Chinese with English abstract). doi:10.1007/BF02873097

Qian, Q., and Li, K. Y. (1996). The Geological Time of Basalt and Strata in North Jiangsu Basin. *Volcanol. Mineral. Resour.* 17, 86–93. (in Chinese with English abstract).

Qiu, H., and Jiang, Y. (2007). Sphalerite 40Ar/39Ar Progressive Crushing and Stepwise Heating Techniques. *Earth Planet. Sci. Lett.* 256, 224–232. doi:10.1016/j.epsl.2007.01.028

Qiu, J. S., Wang, D. Z., and Zhou, J. C. (1999). Geochemistry and Petrogenesis of the Late Mesozoic Bimodal Volcanic Rocks at Yunshan Caldera, Yongtai Country, Fujian Province. *Acta petrologica Mineralogica* 18, 97–107. (in Chinese with English abstract.

Saccani, E., and Photiades, A. (2005). Petrogenesis and Tectonomagmatic Significance of Volcanic and Subvolcanic Rocks in the Albanide-Hellenide Ophiolitic Melanges. *Isl. Arc* 14, 494–516. doi:10.1111/j.1440-1738.2005.00480.x

Shen, W. Z., Hong, L. F., and Li, W. X. (1999). Study on the Sr-Nd Isotopic Compositions of Granitoids in SE China. *Geol. J. China Univ.* 5, 22–32. (in Chinese with English abstract). doi:10.1007/BF02885998

Shervais, J. W. (1982). Ti-V Plots and the Petrogenesis of Modern and Ophiolitic Lavas. *Earth Planet. Sci. Lett.* 59, 101–118. doi:10.1016/0012-821x(82)90120-0

Sun, S.-s., and Mcdonough, W. F. (1989). Chemical and Isotopic Systematics of Oceanic Basalts: Implications for Mantle Composition and Processes. *Geol. Soc. Lond. Spec. Publ.* 42, 313–345. doi:10.1144/gsl.sp.1989.042.01.19

Tang, L. M., Chen, H. L., Dong, C. W., Shen, Z. Y., Cheng, X. G., and Fu, L. L. (2010). Late Mesozoic Tectonic Extension in SE China: Evidence from the Basic Dike Swarms in Hainan Island, China. *Acta Petrol. Sin.* 26, 1204–1216. (in Chinese with English abstract). doi:10.1016/j.sedgeo.2010.03.004

Tatsumoto, M., Basu, A. R., Wankang, H., Junwen, W., and Guanghong, X. (1992). Sr, Nd, and Pb Isotopes of Ultramafic Xenoliths in Volcanic Rocks of Eastern China: Enriched Components EMI and EMII in Subcontinental Lithosphere. *Earth Planet. Sci. Lett.* 113, 107–128. doi:10.1016/0012-821x(92)90214-g

Wang, D. Y., Xu, W. L., Feng, H., Lin, J. Q., and Zheng, C. Q. (2002). Nature of Mesozoic Lithospheric Mantle in Western Liaoning Province: Evidences from Basalt and the Mantle-Derived Xenoliths. *J. Jilin Univ. (Earth Sci. Ed.* 32, 319–324. (in Chinese with English abstract). doi:10.13278/j.cnki.jjuese.2002.04.002

Wang, D. Z., and Shen, W. Z. (2003). Genesis of Granitoids and Crustal Evolution in Southeast China. *Earth Sci. Front.* 10, 209–220. (in Chinese with English abstract).

Wang, R. J., and Yang, S. R. (1987b). On the Evolution and Mineral Chemistry of Olivine, Pyroxene, Plagioclase in Cenozoic Basalts from the Chenxian-Xinchang Basin in Zhejiang Province. *Acta Petrol. Sin.* 2, 27–39. (in Chinese with English abstract).

Wang, R. J., and Yang, S. R. (1987a). The Study of Cenozoic Basalts and its Xenolithos in Shengxian Area, Zhejiang Province. *Earth Sci. J. Wuhan Geol. Coll.* 12, 241–248. (in Chinese).

Wang, S. X. (1998). Discussion of the Chemical Composition of Different-Time Basalt Series and its Formation Environment in Fujian Province. *Geol. Fujian* 18, 68–80. (in Chinese with English abstract).

Wang, X.-C., Li, Z.-X., Li, X.-H., Li, J., Liu, Y., Long, W.-G., et al. (2012). Temperature, Pressure, and Composition of the Mantle Source Region of Late Cenozoic Basalts in Hainan Island, SE Asia: a Consequence of a Young Thermal Mantle Plume Close to Subduction Zones? *J. petrology* 53, 177–233. doi:10.1093/petrology/egr061

Xia, Q. K., Xing, L. B., Feng, M., Liu, S. C., Yang, X. Z., and Hao, Y. T. (2010). Water Content and Element Geochemistry of Peridotite Xenoliths Hosted by Early-Jurassic Basalt in Ningyuan, Hunan Province. *Acta Petrologica Mineralogical* 29, 113–124. (in Chinese with English abstract). doi:10.3724/SP.J.1084.2010.00199

Xiao, L., Zhou, H. M., Dong, Y. X., Zeng, G. C., and Wang, F. Z. (2006). Geochemistry and Petrogenesis of Cenozoic Volcanic Rocks from Sanshui Basin: Implications for Spatial and Temporal Variation of Rock Types and Constraints on the Formation of South china Sea. *Geotect. Metallogenia* 30, 72–81. (in Chinese with English abstract). doi:10.1007/s11442-006-0415-5

Xie, G. Q., Mao, J. W., Hu, R. Z., Li, R. L., and Cao, J. (2005). Discussion on Some Problems of Mesozoic and Cenozoic Geodynamics of Southeast China. *Geol. Rev.* 51, 613–620. (in Chinese with English abstract).

Xie, X., Xu, X. S., Zou, H. B., and Xing, G. F. (2001). Trace Element and Nd-Sr-Pb Isotope Studies of Mesozoic and Cenozoic Basalts in Coastal Area of SE China. *Acta Petrol. Sin.* 17, 617–628. (in Chinese with English abstract).

Xing, G. F., Yang, Z. L., and Tao, K. Y. (1999). Sources of Cretaceous Bimodal Volcanic Rocks in the Coastal Region of Southeastern China-Constraints of the Sr Conten and its Isotopes. *Acta Geol. Sin.* 73, 84–92.

Xu, W. L., Zhou, Q. J., and YangYang, D. B. J. H. (2013). Timing, Style and Process of Modifying Adjacent Lithospheric Mantle by Melts Derived from Deeply Subducted Continental Crust: Evidence from Peridotite and Pyroxenite Xenoliths in Western Shandong. Chinese. *Sci. Bull.* 58, 2300–2305. (in Chinese with English abstract).

Xu, X., Griffin, W. L., O'Reilly, S. Y., Pearson, N. J., Geng, H., and Zheng, J. (2008). Re-Os Isotopes of Sulfides in Mantle Xenoliths from Eastern China: Progressive Modification of Lithospheric Mantle. *Lithos* 102, 43–64. doi:10.1016/j.lithos.2007.06.010

Xu, X. S., and Xie, X. (2005). Late Mesozoic-Cenozoic Basaltic Rocks and Crust-Mantle Interaction, SE China. *Geol. J. China Univ.* 11, 318–334. (in Chinese with English abstract).

Xue, H. M., Tao, K, Y., and Shen, J. L. (1996). Sr and Nd Isotopic Characteristics and Magma Genesis of Mesozoic Volcanic Rocks along the Coastal Region of Southeastern china. *Acta Geol. Sin.* 70, 35–47. (in Chinese with English abstract). doi:10.1111/j.1755-6724.1996.mp9003004.x

Yan, J., Chen, J. F., Xie, Z., Gao, T. S., Foland, K. A., Zhang, X. D., et al. (2005a). Studies on Petrology and Geochemistry of the Later Cretaceous Basalts and Mantle-Derived Xenoliths from Eastern Shandong. *Acta Petrol. Sin.* 219, 99–112. (in Chinese with English abstract).

Yan, J., Chen, J. F., Xie, Z., Yang, G., Yu, G., and Qian, H. (2005b). Geochemistry of Late Mesozoic Basalt from Kedoushan in Middle and Lower Yangtze Regions: Constraints on Characteristics and Evolution of the Lithospheric Mantle. *Geochemica* 34, 455–469. (in Chinese with English abstract).

Yan, J., Chen, J. F., Yu, G., Qian, H., and Zhou, X. (2003). Pb Isotopic Characteristics of Late Mesozoic Mafic Rocks from the Lower Yangtze Region: Evidence for Enriched Mantle. *Geol. J. China Univ.* 9, 195–206. (in Chinese with English abstract).

Yan, Q. S., Shi, X. F., Wang, K. S., and Bu, W. R. (2007). Mineral Chemistry and its Genetic Significance of Olivine in Cenozoic Basalts from the South China Sea. *Acta Petrol. Sin.* 23, 2981–2989. (in Chinese with English abstract). doi:10.1631/jzus.2007.B0900

Yang, G. C., Yang, X. Z., Hao, Y. T., and Xia, Q. K. (2012). Water Content Difference between Continental Lower Crust and Lithospheric Mantle: Granulite and Peridotite Xenoliths Hosted in Basalts from Junan, Shandong Province. *Acta Petrologica Mineralogica* 31, 691–700. (in Chinese with English abstract). doi:10.1007/s11783-011-0280-z

Yang, X.-Z., Xia, Q.-K., Deloule, E., Dallai, L., Fan, Q.-C., and Feng, M. (2008). Water in Minerals of the Continental Lithospheric Mantle and Overlying Lower Crust: A Comparative Study of Peridotite and Granulite Xenoliths from the North China Craton. *Chem. Geol.* 256, 33–45. doi:10.1016/j.chemgeo.2008.07.020

Yang, Z. L., Shen, W. Z., Tao, K. Y., and Shen, J. L. (1999). Sr, Nd and Pb Isotopic Characteristics of Early Cretaceous Basaltic Rocks from the Coast of Zhejiang and Fujian: Evidences for Ancient Enrichied Mantle Source. *Sci. Geol. Sin.* 34, 59–67. (in Chinese with English abstract).

Ying, J.-F., Zhang, H.-F., and Tang, Y.-J. (2010). Lower Crustal Xenoliths from Junan, Shandong Province and Their Bearing on the Nature of the Lower Crust beneath the North China Craton. *Lithos* 119, 363–376. doi:10.1016/j.lithos.2010.07.015

Ying, J. F., Zhang, H. F., Zhou, X. H., and Tang, Y. J. (2013). Tectonic Affinity of the Sub-continental Lithosphere of the Sulu Orogenic Belts: Constraints from Granulite and Peridotites Xenoliths. *Bull. Mineralogy, Petrology Geochem.* 32, 328–334. (in Chinese with English abstract).

Yu, Y. W., Zhou, T. X., and Chen, J. F. (1993). The Characteristics and Genesis of Early Cretaceous Bimodal Volcanic Rocks in Xuantandi Area, Zhejiang Province. *J. Nanjing Univ. Nat. Sci.* 5, 420–429. (in Chinese with English abstract).

Zeng, L., Gao, L.-E., Dong, C., and Tang, S. (2012). High-pressure Melting of Metapelite and the Formation of Ca-Rich Granitic Melts in the Namche Barwa Massif, Southern Tibet. *Gondwana Res.* 21, 138–151. doi:10.1016/j.gr.2011.07.023

Zhang, B. T., Chen, P. R., Ling, H. F., and Kong, X. G. (2004). Pb-Nd-Sr Isotopic Study of the Middle Jurassic Basalts in Southern Jiangxi Province: Characteristic of Mantle Source and Tectonic Implication. *Geol. J. China Univ.* 10, 145–156. (in Chinese with English abstract). doi:10.1142/9789812565839_0011

Zhang, H. F., Zhou, X. H., Fan, W. M., Sun, M., Guo, F., Ying, J. F., et al. (2005). Nature, Composition, Enrichment Processes and its Mechanism of the Mesozoic Lithospheric Mantle beneath the Southeastern North China Craton. *Acta Petrol. Sin.* 21, 1271–1280. (in Chinese with English abstract). doi:10.1016/j.sedgeo.2005.05.009

Zhang, J. C., and Lu, Q. D. (1997). On the Characteristics and Origin of the Cenozoic Basalts in Fujian Province. *Geol. Fujian* 1, 1–9. (in Chinese with English abstract).

Zhang, W., and Fang, N. Q. (2014). Geochemistry Characteristics of Eocene Volcanic Rocks in Sanshui Basin, Guangdong. *Earth Science-Journal China Univ. Geosciences* 39, 37–44. (in Chinese with English abstract). doi:10.4028/www.scientific.net/AMM.275-277.322

Zhang, X. Q., Zhou, X. P., and Chen, X. Y. (1993). *The Atlas of Cretaceous-Paleogene Drilling Stratigraphic in Sanshui Basin*. Beijing: China ocean Press, 183. (in Chinese).

Zhao, J.-H., and Zhou, M.-F. (2007). Geochemistry of Neoproterozoic Mafic Intrusions in the Panzhihua District (Sichuan Province, SW China): Implications for Subduction-Related Metasomatism in the Upper Mantle. *Precambrian Res.* 152, 27–47. doi:10.1016/j.precamres.2006.09.002

Zheng, C. Q., Xu, W. L., and Wang, D. Y. (1999). The Petrology and Mineral Chemistry of the Deep-Seated Xenoliths in Mesozoic Basalt in Fuxin District from Western Liaoning. *Acta Petrol. Sin.* 15, 616–622. (in Chinese with English abstract).

Zhi, X. C., Chen, D. G., Zhang, Z. Q., and Wang, J. H. (1994). Neodymium and Strontium Isotopic Compositions for Later Tertiary Alkalic Basalts from Liuhe-Yizheng, Jiangsu Province, China. *Acta Petrol. Sin.* 10, 383–390. (in Chinese with English abstract).

Zhi, X. C., and Qin, X. (2004). Re-Os Isotope Geochemistry of Mantle-Derived Peridotite Xenoliths from Eastern China: Constraints on the Age and Thinning of Lithosphere Mantle. *Acta Petrol. Sin.* 20, 989–998. (in Chinese with English abstract). doi:10.2116/analsci.20.717

Zhou, J. C., and Chen, R. (2001). Late Mesozoic Interaction between Crust and Mantle in Coastal Area of Zhejiang-Fujian. *Prog. Nat. Sci.* 10, 714–717. doi:10.2183/pjab.76.97

Zhou, Q. J., Xu, W. L., Yang, D. B., Pei, F. P., Wang, W., Yuan, H. L., et al. (2013). Modification of the Lithospheric Mantle by Melt Derived from Recycled Continental Crust Evidenced by Wehrlite Xenoliths in Early Cretaceous High-Mg Diorites from Western Shandong. *Sci. China (Earth Sci.* 43, 1179–1194. (in Chinese with English abstract). doi:10.1007/s11430-012-4533-x

Zhou, Q., Wu, F. Y., Chu, Z. Y., and Ge, W. C. (2010). Isotopic Compositions of Mantle Xenoliths and Age of the Lithospheric Mantle in Yitong, Jilin Province. *Acta Petrol. Sin.* 26, 1241–1264. (in Chinese with English abstract).

Zhou, X. H. (1992). "The Discovery of Cenozoic Transition Series Basalts: the Study of its Geochemical Characteristics and Genesis," in *The Chronology and Geochemistry of Cenozoic Volcanic Rocks in China*. Editor U. R. X. Li (Beijing: Earthquake Press), 285–297. (in Chinese).

Zhou, X., Sun, T., Shen, W., Shu, L., and Niu, Y. (2006). Petrogenesis of Mesozoic Granitoids and Volcanic Rocks in South China: a Response to Tectonic Evolution. *Episodes* 29, 26–33. doi:10.18814/epiiugs/2006/v29i1/004

Zhu, B. Q., Wang, H. F., Mao, C. X., Zhu, N. J., Huang, R. S., Peng, J. H., et al. (1991). Geochonology and Nd-Sr-Pb Isotopic Evidence for Mantle Source in the Ancient Subduction Zone beneath Sanshui Basin, Guangdong Province, China. *Geochemica* 1, 27–32. (in Chinese with English abstract). doi:10.1007/bf02842215

Zou, H., Zindler, A., Xu, X., and Qi, Q. (2000). Major, Trace Element, and Nd, Sr and Pb Isotope Studies of Cenozoic Basalts in SE China: Mantle Sources, Regional Variations, and Tectonic Significance. *Chem. Geol.* 171, 33–47. doi:10.1016/s0009-2541(00)00243-6

Conflict of Interest: The authors declare that the research was conducted in the absence of any commercial or financial relationships that could be construed as a potential conflict of interest.

Publisher's Note: All claims expressed in this article are solely those of the authors and do not necessarily represent those of their affiliated organizations, or those of the publisher, the editors and the reviewers. Any product that may be evaluated in this article, or claim that may be made by its manufacturer, is not guaranteed or endorsed by the publisher.

Copyright © 2022 Li, Zhao, Jiang, Xing, Yu and Duan. This is an open-access article distributed under the terms of the Creative Commons Attribution License (CC BY). The use, distribution or reproduction in other forums is permitted, provided the original author(s) and the copyright owner(s) are credited and that the original publication in this journal is cited, in accordance with accepted academic practice. No use, distribution or reproduction is permitted which does not comply with these terms.